J. Phycol. *, ***–*** (2020)

DOI: 10.1111/jpy.12990

LIMITED GENETIC CONNECTIVITY AMONG *SARGASSUM HORNERI* (PHAEOPHYCEAE) POPULATIONS IN THE CHINESE MARGINAL SEAS DESPITE THEIR HIGH DISPERSAL CAPACITY[1]

*Jing-Jing Li**

College of Oceanography, Institute of Marine Biology, Hohai University, No.1 Xikang Road, Nanjing 210098, China

*Zheng-Yi Liu**, *Zhi-Hai Zhong*, *Long-Chuan Zhuang*

Yantai Institute of Coastal Zone Research, Chinese Academy of Sciences, 17 Chunhui Road, Yantai 264003, China

Yuan-Xin Bi

Key Laboratory of Sustainable Utilization of Technology Research for Fishery Resource of Zhejiang Province, Marine Fisheries Research Institute of Zhejiang Province, Zhoushan 316021, China

and Song Qin[2]

Yantai Institute of Coastal Zone Research, Chinese Academy of Sciences, 17 Chunhui Road, Yantai 264003, China

***Sargassum horneri* is a habitat-forming species in the Northwest Pacific and an important contributor to seaweed rafts. In this study, 131 benthic samples and 156 floating samples were collected in the Yellow Sea and East China Sea (ECS) to test the effects of seaweed rafts on population structure and connectivity. Our results revealed high levels of genetic diversity in both benthic and floating samples based on concatenated mitochondrial markers (*rpl*5-*rps*3, *rnl-atp*9, and *cob-cox*2). Phylogenetic analyses consistently supported the existence of two lineages (lineages I and II), with divergence dating to *c.* 0.692 Mya (95% HPD: 0.255–1.841 Mya), indicating that long-term isolation may have occurred during the mid-Pleistocene (0.126–0.781 Mya). Extended Bayesian skyline plots demonstrated a constant population size over time in lineage I and slight demographic expansion in lineage II. Both lineages were found in each marginal sea (including both benthic and floating samples), but PCoA, F_{ST}, and AMOVA analyses consistently revealed deep genetic variation between regions. Highly structured phylogeographic pattern supports limited genetic connectivity between regions. IMA analyses demonstrated that asymmetric gene flow between benthic populations in the North Yellow Sea (NYS) and ECS was extremely low (ECS→NYS, $2Nm = 0.6$), implying that high dispersal capacity cannot be assumed to lead to widespread population connectivity, even without dispersal barriers. In addition, there were only a few shared haplotypes between benthic and floating samples, suggesting the existence of hidden donors for the floating masses in the Chinese marginal seas.**

Key index words: **biogeography; floating seaweeds; gene flow; golden tide; population connectivity; *Sargassum horneri***

***Abbreviations*: AMOVA, analysis of molecular variance; BI, Bayesian inference; COB, *cob-cox*2 region; EBSPs, Extended Bayesian skyline plots**
ECSEast China Sea; ML, maximum-likelihood; NYS, North Yellow Sea; PCoA, principal component analysis; RPL, *rpl*5-*rps*3 region; RNL, *rnl-atp*9 region; SYS, South Yellow Sea; YS, Yellow Sea

Sargassum horneri, a large conspicuous brown seaweed, is abundant in subtidal areas in the Northwest Pacific (Uwai et al. 2009, Hu et al. 2011). *Sargassum horneri* is native to the eastern Asian coasts and is invasive in the western coasts of North America (Uwai et al. 2009, Kaplanis et al. 2016). The first reported invasive event occurred in Long Beach Harbor in North America in 2003 (Miller et al. 2007) and then quickly spread throughout the coasts of San Diego County (Kaplanis et al. 2016). Moreover, satellite data showed that large patches of floating *S. horneri,* first found near Zhejiang Province waters, were annually transported with the Kuroshio Current to southern Korea and Japan (Komatsu et al. 2007). However, from November 2016 to April 2017, large-scale *S. horneri* biomass (also called a golden tide) accumulated in the East China Sea (ECS) and the Yellow Sea (YS; Zhang et al. 2019). Massive floating biomass was stranded on the *Pyropia* aquaculture rafts, which caused substantial economic damage to the nori industry in this region (Liu et al. 2018). Unlike the naturally

[1]Received 15 October 2019. Accepted 6 March 2020.
[2]Author for correspondence: e-mail sqin@yic.ac.cn.
*Equally contributing authors.
Editorial Responsibility: C. Amsler (Associate Editor)

pelagic *Sargassum* in the Sargasso Sea, *S. horneri* need to attach to a rocky substrate, other seaweeds and/or shells during their early stage, and then the thalli are detached by strong waves and/or grazer activity (Duffy et al. 2019). *Sargassum horneri* have a high acclimation capacity to the changing environment and can perform rapid vegetative growth in an unattached form, which enables them to maintain a large biomass on the sea surface and to colonize new places (Xu et al. 2018).

Floating thalli can stay on the sea surface for months (Fraser et al. 2018), and act as dispersal vectors for hitchhiking mesoherbivores and epiphytes and provide shelter for juvenile fishes, resulting in connectivity of the coastal ecology (Fraser et al. 2013, Guillemin et al. 2014). Long-distance dispersal evaluated by molecular data has been reported in most floating seaweeds such as *Macrocystis pyrifera* (Macaya and Zuccarello 2010) and *Durvillaea antarctica* (Fraser et al. 2018), as well as in hitchhiking seaweeds such as *Adenocystis utricularis* (Fraser et al. 2013), *Capreolia implexa* (Boo et al. 2014), and *Agarophyton* (*Gracilaria*) *chilensis* (Guillemin et al. 2014). Thus, the floating ability and routes of seaweed rafts have attracted wide interest (Rothäusler et al. 2015, Fraser et al. 2018, Tala et al. 2019).

Rafted seaweeds must remain reproductively viable in surface conditions for dispersal to potentially be effective (Xuereb et al. 2018, van Hees et al. 2019). The worldwide invader *Sargassum muticum* has multiple facilitating life-history traits, such as microscopic and dispersive stages, high fecundity, and uniparental reproduction (Le Cam et al. 2019). Similarly, van Hees et al. (2019) demonstrated that rafted *Sargassum spinuligerum* were photosynthetically and reproductively identical to benthic individuals, thereby increasing the dispersal longevity of viable progeny. *Macrocystis pyrifera* can disperse over distances up to 1000 km with viable propagules (Hernández-Carmona et al. 2006). However, Pang et al. (2018) reported that the number of spermatophores in each male receptacle in floating *S. horneri* thalli is much lower than that in epilithic thalli during the same season in the same area. So the genetic connectivity of *S. horneri* may be much lower than previously assumed.

Successful colonization via algal rafting is affected by a broad variety of abiotic factors including hydrological/geographic barriers, ocean currents, and environmental gradients (Saunders 2014, Tala et al. 2019). The Chinese marginal seas are characterized by intricate oceanic currents, which have profound effects on the population expansion and vicariance of coastal species (Li et al. 2017a). Complex interactions between winds, currents, and eddies determine the dispersal trajectories of seaweed rafts (Komatsu et al. 2014b, Rothäusler et al. 2015). During spring and early summer, the China Coast Current that flows northward is dominant in the ECS and YS, but in winter, the China Coast Current flows southwards, which may facilitate the mixture of lineages (Hu et al. 2011). But some studies showed that Changjiang diluted water could act as physical barriers to reduce genetic exchange of marine species between ECS and YS (Ni et al. 2014, Li et al. 2017b). Thus, co-distributed species, which are characterized by different dispersal potential and stress tolerances, tend to have contrasting phylogeographic patterns (Wang et al. 2015).

The Chinese marginal seas have been through dramatic changes of sea level caused by Pleistocene climate oscillations (Benzie and Williams 1997, Hu et al. 2015). Seaweeds along the coast of China have experienced multiple range contractions and expansions, leading to dynamic phylogeographic signatures in the present populations (Ni et al. 2014). Coastal species in this region are often characterized by multiple lineages (e.g., *Cellana toreuma*; Dong et al. 2012), *Sargassum thunbergii* (Li et al. 2017b), and *Sargassum fusiforme* (Hu et al. 2017). Postglacial dispersal conducted by coastal currents and/or wind strongly influences population connectivity, keeping or diluting the genetic variation left by past climates (Fraser et al. 2013, Provan 2013). Thus, positive buoyant seaweeds in this region are ideal models to illustrate how contemporary gene flow shapes phylogeographic patterns.

Several studies have investigated the genetic diversity and population structure of *Sargassum horneri* along the Chinese coasts. For example, Hu et al. (2011) revealed a shallow genetic substructure in eight benthic *S. horneri* populations based on mtDNA *cox*3 data, which may have resulted from late Pleistocene demographic expansion and the absence of physical barriers to dispersal. Su et al. (2017) sampled 271 *S. horneri* individuals from seven locations in China and two locations in Korea. The results showed that significant genetic variation was found among most of the populations based on microsatellite data and that the floating *S. horneri* populations that occurred in different years may originate from multiple sources. Liu et al. (2018) sampled 196 floating *S. horneri* thalli from the YS and detected two genetic clusters that coexisted in each sampling site. These results have greatly enhanced our understanding of the genetic diversity distribution pattern of *S. horneri* on the Chinese coasts, but whether population connectivity is facilitated by seaweed rafts along the Chinese coasts is much less explored.

In this study, a total of 20 *Sargassum horneri* populations were collected in the YS and ECS, including 131 benthic samples and 156 floating samples. MtDNA markers (*rnl-atp*9, *rpl*5-*rps*3, and *cob-cox*2) were used to investigate the genetic variability and population connectivity of *S. horneri* and to evaluate the impacts of floating mats on population connectivity.

MATERIALS AND METHODS

Sample collection. A total of 287 *Sargassum horneri* samples (including 131 benthic samples and 156 floating samples) were collected from 20 sites in the Yellow Sea (YS) and East China Sea (ECS), covering most of the distribution range in this region (Fig. 1, Table S1 in the Supporting Information). Based on our field investigation, *S. horneri* forests are generally found from 2 to 5 m in depth; thus, benthic samples were mainly collected at depths of 2–5 m by scuba divers using dive knives. At each location, individuals were collected at an interval of at least 2 m to reduce the likelihood of collecting related plants. As no benthic individuals grow in the coasts of the South Yellow Sea (SYS), we only sampled benthic individuals in the North Yellow Sea (NYS) and ECS.

Floating *Sargassum horneri* were collected with ring nets on fishing boats, and/or manually on aquaculture ropes and beaches (Table S1). During the navigation (>50 km from the coastline), 1–6 individuals of *S. horneri* in a single patches (>60 cm in diameter) were collected. Additional floating samples were collected from individuals stranded on aquaculture ropes and from beaches at an interval of at least 2 m to reduce the likelihood of collecting the same individual. Floating thalli have no holdfast and higher density of vesicles than benthic thalli (Zhu et al. 2019). Leaf tips of 5–10 cm were dried and stored in silica gel for the following molecular analyses.

DNA extraction and amplification. Total genomic DNA was extracted using a Plant Genomic DNA Extraction Kit (Tiangen Biotech. Co. Ltd., Beijing, China) according to the manufacturer's instructions. Mitochondrial *rnl-atp9* (RNL), *rpl5-rps3* (RPL), and *cob-cox2* (COB) regions were amplified using primers published in Liu et al. (2018), which have been verified to be efficient to illustrate the population variation of *Sargassum horneri*. The PCR profile included denaturation at 94°C for 5 min; denaturation at 94°C for 30 s, annealing at 50°C for 35 s, and extension at 72°C for 1 min, 35 cycles; then extension at 72°C for 10 min. Sequencing reactions were performed from both sides using an ABI 3730 XL DNA analyzer (Applied Biosystems, Foster City, CA, USA) by Sangon Biotech (Shanghai, China) Co, Ltd.

Molecular diversity and phylogeographic structure. Sequences were aligned and trimmed using CLUSTAL X (Thompson et al. 1997) and BioEdit 7.053 (Hall 1999), respectively. Genetic diversity parameters, including haplotype distribution, number of haplotypes (N_h), private haplotypes (H_p), haplotype diversity (h), and nucleotide diversity (π) were estimated in Arlequin 3.5 (Excoffier and Lischer 2010). A parsimony median-joining network was generated to evaluate the relationships among haplotypes with the program Network 4.5.1 (Bandelt et al. 1999), and MODELTEST 3.7 (Posada and Crandall 1998) was used to identify the best substitution model for each locus under the Bayesian information criterion (BIC) (RPL: GTR+I, I = 0.505; RNL: HKY85+I,

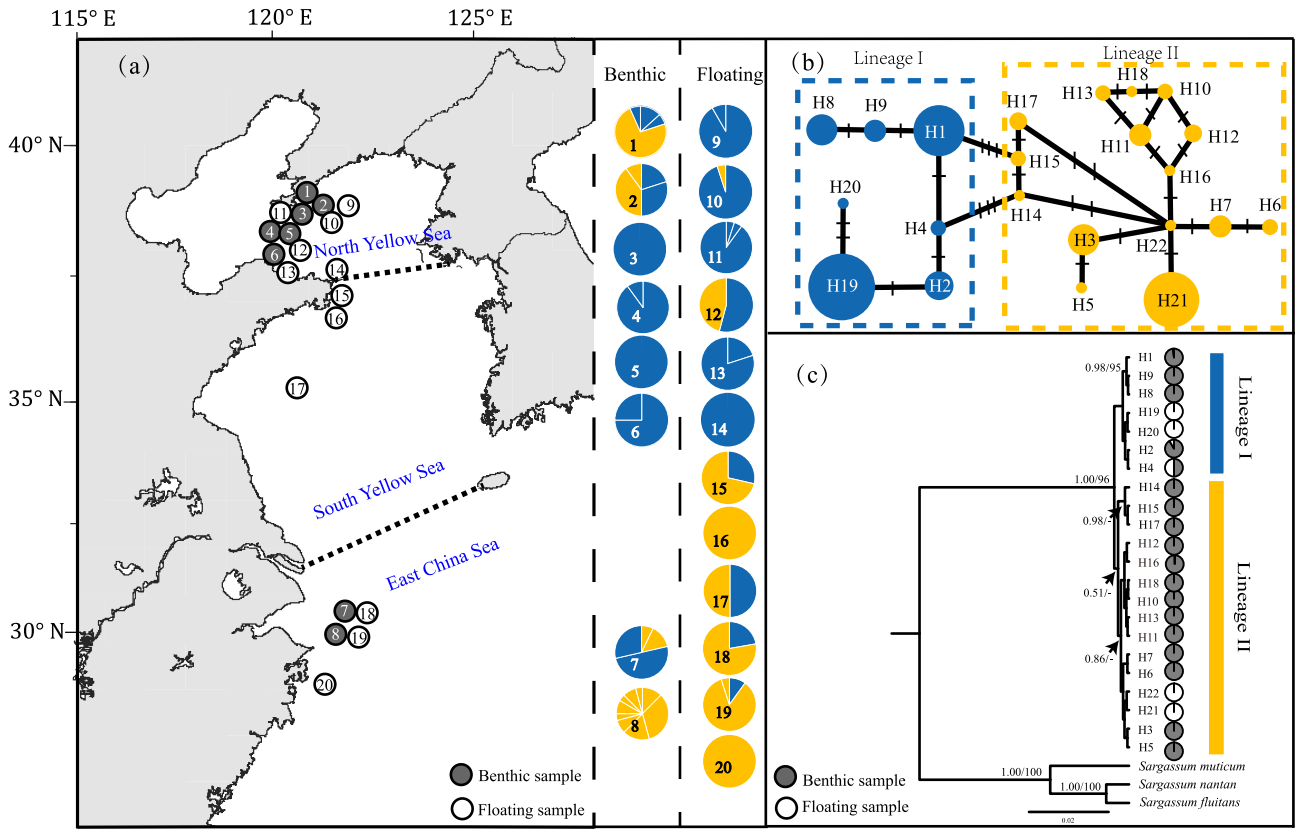

FIG. 1. (a) Haplotype distribution pattern of *Sargassum horneri* in the Yellow Sea and East China Sea inferred from mitochondrial RPL+RNL+COB data. Numbers in the pie chart correspond to the sampling localities in Table S1. (b) Median-joining network inferred from concatenated mitochondrial data. The size of each circle is proportional to the frequency of haplotypes and each line between main haplotype represents one mutation step. (c) Rooted Bayesian inference (BI, upper)/maximum-likelihood (ML, lower) trees (only values higher than 0.50/50 are shown) inferred from mitochondrial data. The pie graph near each haplotype represents the proportion of benthic and floating samples.

I = 0.683; COB: GTR+G, G = 0.380; RPL+RNL+COB: GTR+G, G = 0.28). Phylogeographic trees were constructed with maximum-likelihood (ML) and Bayesian inference (BI) methods. The congeneric species *Sargassum natans* (GenBank accession no. KY084907.1), *S. fluitans* (no. KY084909.1), and *S. muticum* (no. KJ938301.1) were chosen as outgroups. ML trees were constructed using the selected model for each marker with 100 bootstrap replicates in PhyML 3.0 (Guindon et al. 2010). For BI analysis, Bayesian searches performed in MrBayes 3.2 (Ronquist et al. 2012) included four chains, and each chain was run for one million generations with a tree sampling frequency of every 100 generations, with the first 10% of the resulting trees discarded as burn-in.

Pairwise genetic differentiation was measured using F_{ST} (Excoffier et al. 2009) in Arlequin 3.5. Analysis of molecular variance (AMOVA) conducted in Arlequin was used to assess the spatial partitioning of genetic variance among the groups. Groups were defined as the following: (I) sampling state, benthic (Pop 1–8) and floating (Pop 9–20) populations; (II) marginal seas, NYS (Pop 1–6, 9–14) and SYS/ECS (Pop 7–8, 15–20); and (III) sampling state and marginal seas (Pop 1–6; Pop 9–14; Pop 7–8; Pop 15–20). To test genetic distinctiveness of populations, principal component analysis (PCoA) was conducted in Genalex (Peakall and Smouse 2012) based on concatenated mitochondrial markers (RPL+RNL+COB).

Gene flow and lineage divergence time. The isolation-with-migration model implemented in IMa2 (Nielsen and Wakeley 2001, Hey and Nielsen 2007, Hey 2010) was used to estimate migration rates (m), population sizes (Θ), and divergence time (t) of samples based on mtDNA data (running as independent loci). Several runs were conducted to determine the most efficient search parameters that maximized mixing. The final runs included 50 coupled Markov chains, a burn-in period of 100,000 steps, and a geometric heating model, with the first and second heating parameters of 0.99 and 0.94 for individual chains. A total of 100,000 genealogies were sampled to estimate the joint posterior probability distributions of the migration parameters.

The mutation rate of each locus was calculated based on the methods described in Hoarau et al. (2007). Divergence of *Psb*A sequences between *Sargassum horneri* (no. KP8813341) and *Fucus vesicuosus* (no. DQ307679) was 5.4%, and the estimated divergence time was 45.0–67.5 Mya (5.4/0.12 and 5.4/0.08, respectively). Divergence of mtDNA sequences between *S. horneri* and *F. vesiculosus* (AY494079) was 33.9% (RPL), 35.6% (RNL), and 23.4% (COB). Thus, the estimated divergence rate of RPL was 0.502%–0.753% per Myr; the estimated divergence rate of RNL was 0.527%–0.791% per Myr; and the estimated divergence rate of COB was 0.346%–0.520% per Myr. As the mutation rate should be half of the divergence rate, the estimated mutation rates were $2.51–3.77 \times 10^{-9}$, $2.64–3.96 \times 10^{-9}$, and $1.73–2.60 \times 10^{-9}$ substitutions per site per year for RPL, RNL, and COB, respectively. *Sargassum horneri* is shown to have a unimodal growth cycle and to have an annual cycle of growth and regeneration (Yoshida et al. 1998).

Demographic history. Three complementary approaches were used to infer the demographic history of *Sargassum horneri* samples. Initially, Tajima's D (Tajima 1989) and Fu's F_S (Fu 1997) were calculated using Arlequin 3.5 to test departure from population demographic equilibrium. Significant departure from selection-drift equilibrium was tested by 1,000 bootstrap replicates. Under the assumption of neutrality, negative values represent population expansions, while positive values are considered a signature of recent bottlenecks (Excoffier and Lischer 2010). Second, mismatch distributions implemented in Arlequin 3.5, which represent the frequency distribution of pairwise nucleotide differences among all haplotypes within populations, were used to test demographic history (Rogers and Harpending 1992). Multimodal mismatch distributions indicate that populations are in demographic equilibrium, whereas a unimodal distribution represents recent demographic expansion. Third, extended Bayesian skyline plots (EBSPs) were implemented in BEAST v1.7.4 (Bouckaert et al. 2014) to reconstruct the demographic changes over time. Mitochondrial RPL, RNL, and COB data were analyzed using GTR, HKY, and GTR+G substitution models separately, with constant Bayesian skyline tree priors. A strict clock model with a mean estimated mutation rate for each marker was used to convert units of substitution per site to years. Default priors were used for all parameter settings. Independent MCMC runs of 1×10^8 generations and parameters were sampled every 1,000 interactions, with the first 10% of generations discarded as burn-in. The effective sample sizes of important parameters sampled from the MCMC were >200, which were visualized in Tracer v1.5 (http://beast.bio.ed.ac.uk/Tracer).

RESULTS

Genetic diversity and haplotype distribution. MtDNA sequences, including 856 bp of *rpl*5-*rps*3 (RPL), 554 bp of *rnl-atp*9 (RNL), and 791 bp of *cob-cox*2 (COB), were obtained from 287 individuals. The RPL yielded six haplotypes (GenBank accession numbers: MN920472–MN920477) with four polymorphic sites, RNL yielded four haplotypes (GenBank accession numbers: MN920468–MN920471) with three polymorphic sites, and COB yielded seven haplotypes (GenBank accession numbers: MN920461–MN920467) with six polymorphic sites (Table S2 in the Supporting Information). The concatenated RPL+RNL+COB datasets with an aligned length of 2201 bp consisted of 11 polymorphic sites (Table S2), yielding 22 haplotypes from all samples. Of these haplotypes, 16 (72.7%) were found in a single population and six were singletons (haplotypes represented by a single sequence; Table S3 in the Supporting Information). Endemic haplotypes H6–H18 were only found in benthic populations in Dongji Island (B-DJI) and Gouqi Island (B-GQI) in the ECS (Fig. 1, a and b). Haplotype H1 was widely found in benthic populations in the NYS, accounting for 60% of all specimens in this region (Fig. 1, a and b; Table S3). Haplotypes H19 and H21 were found in most floating populations, accounting for 84.6% of floating specimens (Fig. 1a; Table S3). In particular, H19 was dominant in the NYS (83%), and H21 was mainly found in the SYS and ECS (87%; Fig. 1, a and b; Table S3). Benthic populations have 15 private haplotypes compared to 4 private haplotypes in floating populations (Table S3). Haplotypes H1, H2, and H4 were found in both floating and benthic samples, but no haplotypes were shared by benthic populations in the NYS and ECS (Table S3).

The concatenated dataset showed that the genetic diversity of benthic samples ($h = 0.812 \pm 0.028$, $\pi = 0.00136 \pm 0.00080$) was higher than that of floating samples ($h = 0.527 \pm 0.017$, $\pi = 0.00136 \pm 0.00079$; Table S1). Similar results were also

revealed by estimates based on each mtDNA marker, RPL (benthic: $h = 0.698 \pm 0.029$, $\pi = 0.00150 \pm 0.00105$; floating: $h = 0.510 \pm 0.014$, $\pi = 0.00118 \pm 0.00088$), and COB markers (benthic: $h = 0.701 \pm 0.032$, $\pi = 0.00145 \pm 0.00105$; floating: $h = 0.500 \pm 0.014$, $\pi = 0.00125 \pm 0.00094$; Table S4 in the Supporting Information). For benthic populations, Dongji Island (B-DJI), Gouqi Island (B-GQI), and Zhangzi Island (B-ZZB) had the highest genetic diversity ($h = 0.667$–0.855, $\pi = 0.00091$–0.00137; Table S1). For floating samples, Daqin Island (F-CDA), Rongcheng (F-RCB), and the Yellow Sea (F-YLS) showed the highest genetic diversity ($h = 0.476$–1.000, $\pi = 0.00130$–0.00272; Table S1).

Phylogenetics and population structure. The BI/ML trees based on each mtDNA locus (RPL, RNL, and COB) consistently demonstrated two lineages (Fig. S1 in the Supporting Information). RPL and COB analyses consequently showed a genetic split between floating populations in the NYS and SYS/ECS, and homogeneous structure in benthic populations (Fig. S1, b and d). One lineage mainly occurred in floating populations in the NYS and benthic populations, and the other mainly occurred in floating populations in the SYS/ECS. In particular, the RNL haplotype network revealed the presence of two main haplogroups, one for benthic populations and one for floating populations (Fig. S1c). Haplotype networks and phylogenetic trees of all *Sargassum horneri* samples in the Chinese marginal seas were highly structured based on concatenated mtDNA sequences (Fig. 1, b and c). Two well-supported phylogenetic lineages, referred to as lineages I and II, were also inferred from the ML/BI trees based on concatenated mtDNA data (Fig. 1c). In general, lineage I was widely distributed in the NYS, accounting for 79.7% and 85.2% of the benthic and floating samples, respectively (Fig. 1; Table S3); lineage II was commonly found in the SYS and ECS, accounting for 60.5% and 81.5% of the benthic and floating samples, respectively (Fig. 1). However, haplotypes (H3 and H5) in lineage II were widely found in the benthic populations in Dalian (Pop 1 and 2; Fig. 1).

Most F_{ST} values between populations were significant (Table S5 in the Supporting Information). A deep genetic split was detected between benthic and floating samples, with 92% $F_{ST} > 0.250$. In addition, significant genetic divergence was also detected between benthic populations in the NYS (Pop1–6) and ECS (Pop7–8; F_{ST} range = 0.382–0.732). Similarly, floating populations in the NYS (Pop 9–14) were significantly divergent from populations in the SYS (Pop 15–17) and ECS (Pop 18–20; 91.6% $F_{ST} > 0.300$). Most F_{ST} values between floating populations within geographic regions were low and non-significant: NYS (Pop 9–14; F_{ST} range: −0.092 to 0.368) and SYS/ECS (Pop 15–20; F_{ST} range: −0.313 to 0.425; Table S5).

When we divided the samples into benthic and floating groups (scenario I), 24.13% of variation occurred among regions ($\Phi_{CT} = 0.241$, $P < 0.01$) and 45.73% occurred within populations (Table 1). A deep split between populations between marginal seas (scenario II) was also detected ($\Phi_{CT} = 0.331$, $P < 0.001$), and accounted for 33.14% of the variation. Moreover, when we grouped the samples into four regions based on sampling type and location (scenario III), nearly half of the variation occurred among regions ($\Phi_{CT} = 0.484$, $P < 0.0001$; Table 1). For all AMOVA analyses, ~30% of genetic variance consistently occurred within sampling localities (% var = 28.09–30.14, $P < 0.0001$; Table 2). Moreover, genetic variation in *Sargassum horneri* along the coast of China was also supported by PCoA profiling of axis 1 vs axis 2 (Fig. 2a). Significant genetic split was detected between benthic and floating samples based on PCoA profiling of axis 2 vs axis 3 (Fig. 2b).

Demographic history, divergence time, and gene flow. Neutrality tests showed that none of the Tajima's *D* and Fu's *Fs* values estimated for each lineage were significantly negative ($P > 0.05$; Table 2). Multimodal distributions were observed in the mismatch distributions for both lineages (Fig. 3a), rejecting a demographic expansion scenario. For lineage I, EBSPs showed a constant population size over time. For lineage II, EBSPs suggest a slow demographic expansion since 0.150 Mya, followed by a relatively

TABLE 1. Analysis of molecular variance (AMOVA) to partition genetic variance in *Sargassum horneri* populations in Chinese marginal seas under hypothesized substructure components. The group codes are in parentheses, identical to sampling localities in Figure 1.

Among regions			Among populations within regions			Within populations		
df	%var	Φ_{CT}	df	%var	Φ_{SC}	df	%var	Φ_{ST}
I) State (Benthic: Pop1–8; Floating: Pop9–20)								
1	24.13	0.241*	18	45.73	0.602***	267	30.14	0.698***
II) Marginal seas (NYS: Pop1–6, Pop9–14; SYS + ECS: Pop7–8, Pop15–20)								
1	33.14	0.331**	18	38.77	0.580***	267	28.09	0.719***
III) State + Marginal seas II (Pop1–6; Pop7–8; Pop9–14; Pop15–20)								
3	48.39	0.484***	16	21.54	0.417***	267	30.07	0.699***

NYS: North Yellow Sea; SYS: South Yellow Sea; ECS: East China Sea.
***$P < 0.0001$, **$P < 0.001$, *$P < 0.01$.

TABLE 2. Tajima's *D* and Fu's *F*s test of lineage I and II of *Sargassum horneri* in the Chinese marginal seas.

Lineage	Tajima's *D*	*P*	Fu's *F*s	*P*
Lineage I	1.762	0.952	1.654	0.781
Lineage II	−0.178	0.493	−5.277	0.033

stationary period from 0.025 Mya (Fig. 3b). The divergence time between the two lineages was *c.* 0.692 Ma (95% HPD 0.255–1.841 Ma; Fig. 4a).

Based on the sampling localities and genetic lineages, we divided the benthic samples into three groups: populations in Dalian in the NYS (N1), populations in Changdao in the NYS (N2), and populations in Zhoushan in the ECS (E). Pairwise estimate comparisons between groups were conducted to estimate gene flow. Because floating samples may have mixed origin, we excluded these samples from this analysis. There is asymmetrical genetic exchange between populations in the NYS (N1 and N2). The migration rate from N1 to N2 was ~3.178 (95% HPD: 0.54–14.93), and the posterior probability distribution for gene flow in the opposite direction lacked a single clear peak (Fig. 4b). The only detected gene flow between the NYS and ECS was from E to N2 with a value of 0.60 (95% HPD: 0.00–2.74; Fig 4c). For comparisons between N1 and E, the posterior distributions of *m*1 and *m*2 had no clear peak.

DISCUSSION

Considering the high dispersal potential of *Sargassum horneri*, we wondered whether large floating *S. horneri* biomass could affect the population genetic structure of benthic populations in the Chinese marginal seas. Herein, we conducted spatiotemporal sampling and used mitochondrial markers to analyze population structure and connectivity of *S. horneri* in this area. The results revealed deep genetic variation and limited gene low between *S. horneri* populations in YS and ECS, implying that high dispersal capacity cannot be assumed to lead to widespread population connectivity.

Deep genetic lineages and phylogeographic pattern. Mitochondrial markers have been widely used to reveal phylogeographic pattern of *Sargassum* species (Chan et al. 2013, Hu et al. 2017, Li et al. 2017a) due to their fast mutation rates. Hu et al. (2011) revealed a homogeneous structure of *S. horneri* among Chinese marginal seas based on *cox*3 data. However, in our study, two genetic lineages were revealed based on concatenated mtDNA sequences. The two lineages may originate from populations that survived in at least two glacial refugia, as long-term isolation will generate a large number of private haplotypes. Previous studies have inferred several refugia in the Northwest Pacific during glacial periods (e.g., the Okinawa Trough, the South China Sea and the Sea of Japan; Ni et al. 2014, Ng et al. 2019). Multiple lineages were reported in most intertidal species that require a hard substratum in this area, such as the seaweed *Chondrus ocellatus* (Hu et al. 2015) and *S. thunbergii* (Li et al. 2017b), the limpet *Siphonaria japonica* (Wang et al. 2015), and *Cyclina sinensis* (Xu et al. 2009). In addition, both lineages were found in the two marine regimes (YS and ECS), suggesting that secondary contact may have occurred in these areas during postglacial expansion. We did not detect significant demographic expansion in *S. horneri*, which may be the result of founder events and genetic drift that have caused the loss of genetic diversity during postglacial recolonization.

Considering the difficulty of calibrating molecular clocks for sargassacean, which have no fossil record (Hoarau et al. 2007); the mutation rates were estimated indirectly as in Hoarau et al. (2007). These molecular clocks have been widely used to reveal phylogeographic process of marine heterokont seaweed (Muhlin and Brawley 2009, Chan et al. 2013, Ng et al. 2019). Sea-level fluctuations during the Pleistocene resulted in repeated physical isolation of marine organisms in Chinese marginal seas, resulting in intraspecific genetic differentiation (Ni et al. 2014, Li et al. 2017b). In our study, the divergence time between the two *Sargassum horneri* lineages occurred in the mid-Pleistocene (0.692 Ma, 95% HPD: 0.255–1.841 Mya). This is much older than the divergence times between *S. fusiforme* subgroups along the Chinese coasts (0.106–0.128 Mya), but close to the divergence time between clades in the Japan-Pacific coasts (0.756 Mya, 95% HPD: 0.273–1.344 Ma; Hu et al. 2017). The divergence within *S. horneri* occurred more recently than that within *S. hemiphyllum* (0.92–2.88 Mya; Cheang et al. 2010a) in the Northwest Pacific. Thus, phylogeographic history of *Sargassum* species in the Northwest Pacific was structured by different Pleistocene glacial episodes.

"Golden tide" in the Chinese marginal seas. Floating masses of *Sargassum* (represented by *S. natans* and *S. fluitans*), called "golden tides," occur regularly in the Gulf of Mexico, Caribbean and West Africa (Sissini et al. 2017). However, since 2016, the golden tide formed by *S. horneri* has been found to be intensified dramatically in frequency and range on the Chinese coasts (especially the YS and ECS) and the southwestern coast of Korea (Liu et al. 2018, Byeon et al. 2019), perhaps due to coastal eutrophication (Zhang et al. 2019) and sea water warming (Qi et al. 2017). So far, the causes and origins of the large floating biomass remain unknown.

Previous studies based on satellite image data assumed that floating samples in the Chinese marginal seas may originate from Zhoushan Zhejiang (Komatsu et al. 2007, Qi et al. 2017). For example, satellite imagery using a Moderate Resolution Imaging Spectroradiometer showed that seaweeds (brown algae) from Zhejiang Province, appearing every

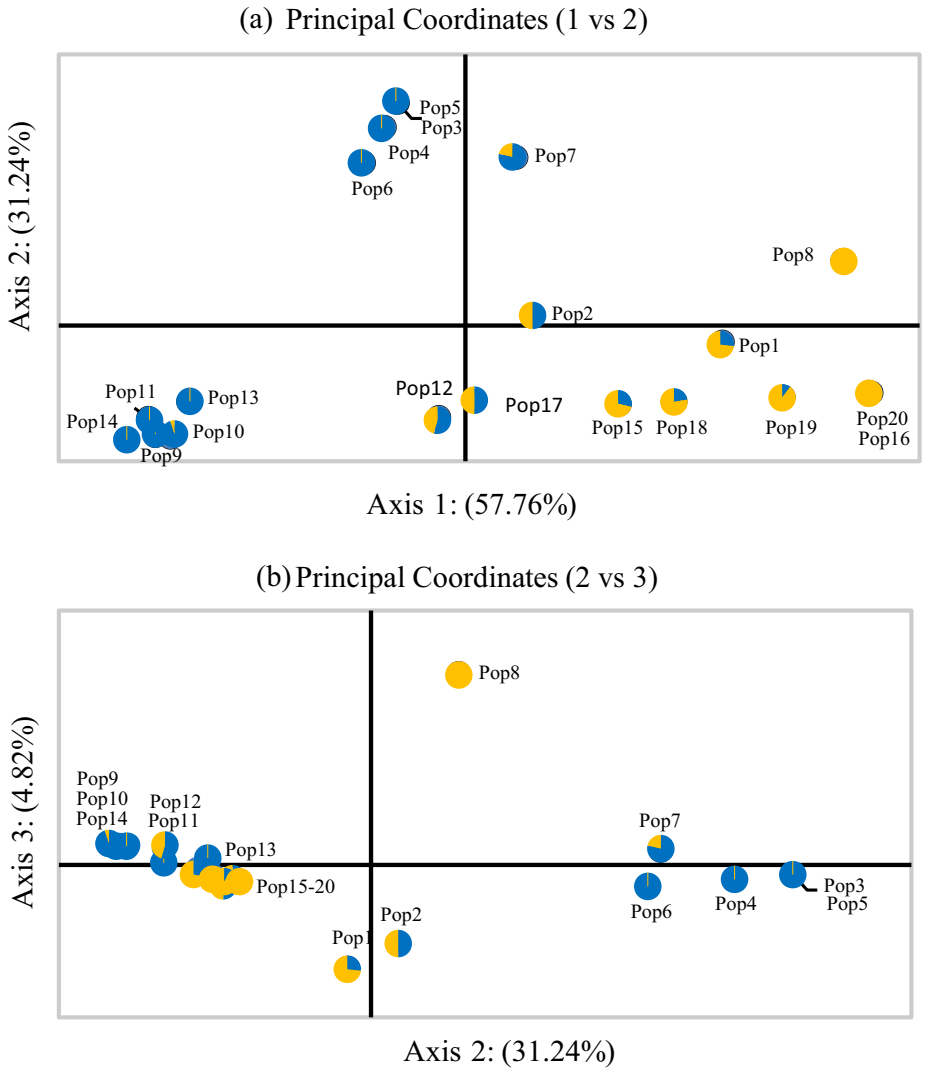

FIG. 2. Principal component analysis (PCoA) of axis 1 versus axis 2 (a) and axis 2 versus axis 3 (b) based on concatenated mtDNA sequences of *Sargassum horneri*. Dark and light colors represent the proportion of lineage I and lineage II, respectively, in each population. The code of populations and lineages are the same as in Figure 1.

February–March since 2012, were transported northeast and finally transported to the YS by the end of April (Qi et al. 2017). A similar trajectory was also demonstrated by Komatsu et al. (2007) using satellite tracking buoys released from the coasts of the Zhejiang Province (118°21′–120°30′ E, 29°11′–30°33′ N). However, in our study, there are no shared haplotypes between benthic populations in Zhoushan (Pop 7 and 8) and all of the floating samples. Thus, we assumed that the donor populations for floating samples in this region may have some unknown habitat (e.g., deeper area and/or aquaculture rafts). On the Sanriku coasts of Japan, *Sargassum horneri* are attached to the bottom to a depth of >7 m and form canopies on the sea surface (Xu et al. 2016). Additionally, Assis et al. (2015) reported that the deeper waters may act as climatic refugia for temperate marine forests to maintain biodiversity, as deeper colder waters would protect species from unfavorable sea surface changes and allow long-term persistence of distinct gene pools. In addition, the biomass of *S. horneri* that attached to the shells and culture rafts in mussel aquaculture area (15.66 km^2) in Zhejiang province was *ca.* 120 $t \cdot km^{-2}$ (calculated in Ding et al. 2019). *Sargassum horneri* became dislodged by waves and human activity (cleaning and mussel harvesting), thus supporting the initial occurrence of golden tides in YS and ECS. Sampling in mussel aquaculture area in Zhejiang province is needed in the future work to verify this assumption.

In our study, high levels of genetic diversity were revealed in both benthic and floating *Sargassum horneri* in the YS and ECS based on mtDNA data. Additionally, the floating samples collected in the SYS and ECS were genetically distinct from the floating

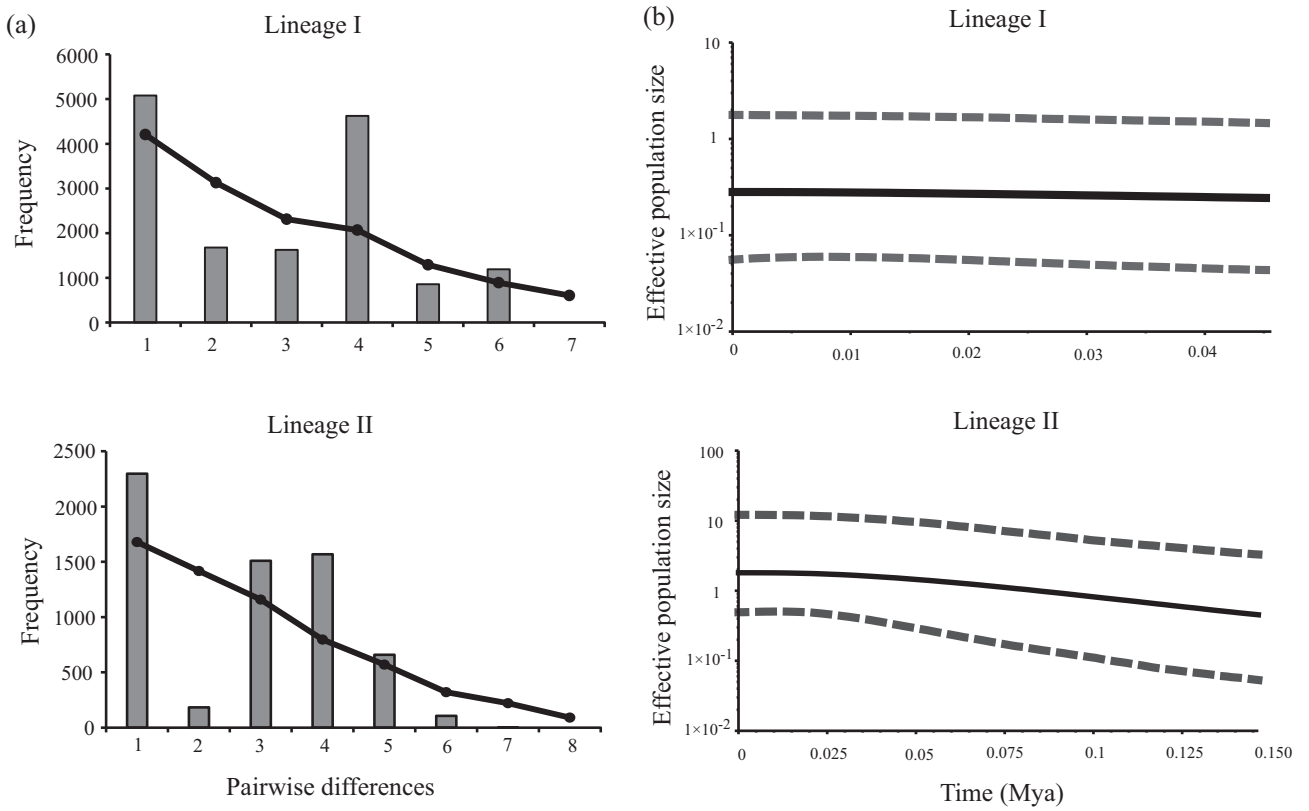

FIG. 3. Mismatch distribution (a) and extended Bayesian skyline plots (EBSPs) (b) of *Sargassum horneri* inferred from the concatenated mtDNA sequences. The upper and lower limits of gray trend represent the 95% highest posterior density intervals.

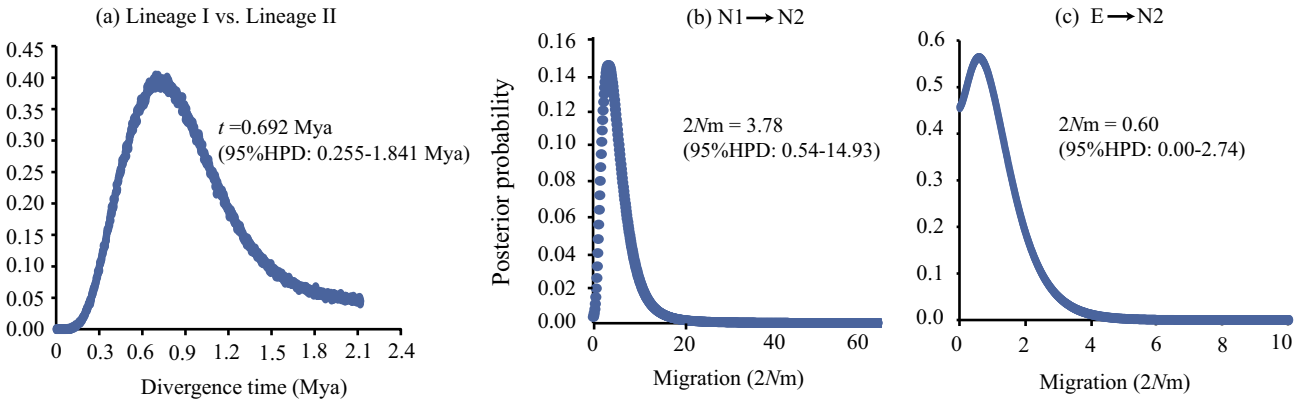

FIG. 4. Estimated marginal posterior density distributions of divergence time between lineages (a) and migration rates (2*N*m) for pairwise populations in different geographic regions [N1→N2 (b) and E→N2 (c)]. Posterior probability distribution lacked a single clear peak are not shown. N1: benthic populations in Dalian in North Yellow Sea (Pop 1–3); N2: benthic populations in Changdao in North Yellow Sea (Pop 4–6); E: benthic populations in East China Sea (Pop 7–8).

samples in the NYS, suggesting multiple and distinct donor populations. Rongcheng (Pop 14–16), located in the border zone of the NYS and SYS, was characterized by a mixture of two lineages. Floating *S. horneri* were often found stranded on aquaculture ropes in Rongcheng from December to May of the following year, which could be regarded as a mixture of colonists in the NYS and SYS. This assumption was also verified by satellite observations: from October to January, the initial site of floating *Sargassum* was found in the YS near the eastern end of the Shandong Peninsula (Rongcheng), and moved southward with the Chinese Coastal Current (Xing et al. 2017); during spring, seaweeds (brown seaweed) were transported northeast and finally transported to the YS by the end of April (Qi et al. 2017).

Limited gene flow between benthic Sargassum horneri *populations.* Deep genetic variation was detected between benthic samples in the NYS and ECS, which was distinct from the assumption that species with high dispersal ability are expected to have panmictic genetic structure (Chan et al. 2013, Grummer et al. 2019). Based on IMA analyses, limited gene flow was detected between populations in the NYS and ECS ($2Nm = 0.6$; Fig. 4), which may be facilitated by the China Coastal Current in the spring and summer. Similarly, Wang et al. (2015) found higher gene flow of *Sargassum horneri* from the ECS to NYS than the southward direction based on *cox*3 data using MIGRATE software. In addition, Yu et al. (2013) found that the genetic differentiation of *S. horneri* populations along the Chinese coasts agreed with the isolation by a distance (IBD) model based on ISSR and SRAP data. This distribution pattern of genetic variation is often represented by species with limited dispersal ability, which has been verified in seaweed *Gelidium canariense* (Bouza et al. 2006), *Ahnfeltiopsis pusilla* (Couceiro et al. 2011), *Fucus ceranoides* (Neiva et al. 2012), and *Mazzaella laminarioides* (Faugeron et al. 2001).

Sargassum horneri can stay on sea surfaces for several months (Yatsuya 2008); thus, geographic distance should not be responsible for the genetic variation. Compared with unoccupied shores, algal rafts have limited potential to enhance gene-flow among established populations (Waters et al. 2013). Along the Chinese coasts, *S. horneri* is not the only canopy-forming species in the marine forest; brown seaweed, *Saccharina japonica* (Zhang et al. 2015), *S. muticum* (Cheang et al. 2010b), and *Undaria pinnatifida* (Epstein and Smale 2017), together compete for suitable rocky shores to grow. Thus, new recruits are less likely to colonize. Moreover, benthic populations in Zhoushan, Zhejiang (Pop 7 and 8) were genetically distinct, suggesting limited population connectivity at a small geographic scale. With the lack of rocky substrate, germlings of floating *S. horneri* could attach to other seaweed instead of rocky substrates (e.g., *Saccharina japonica*). This attachment strength becomes weaker as *S. horneri* grow longer, allowing detached thalli to join the floating patches (field observation).

Insights into seaweed conservation. Despite the detrimental effects of accumulating a large amount of biomass on the sea surface, *Sargassum horneri* play a key role in supporting coastal ecosystem function, including serving as spawning and nursery grounds for various marine species in the marine forest. *Sargassum horneri* forests have experienced a noticeable regression on the Chinese coasts because of habitat destruction, pollution, invasive species, and ocean warming, which may cause the loss of genetic diversity (Harley et al. 2012, Wernberg et al. 2016). High biodiversity increases the survival rates under climate changes (Reusch 2014, Duarte et al. 2018). *Sargassum horneri* harbor multiple genotypes and phenotypes at different geographic scales (Hu et al. 2011, Lin et al. 2017), which is important for them to adapt to environmental variables.

Climate changes, mainly via rising temperature and ocean acidification, have shaped the distribution and abundance of most marine species. Range shifts are expected, as coastal species shift to higher latitudes or greater depth to seek more appropriate habitats (Harley et al. 2012). Komatsu et al. (2014a) predicted that the southern limits of *Sargassum horneri* distribution will move northwards under the A2 scenario of global warming. Thus, genetically unique and high-diversity lineages of *S. horneri* near the edge may be lost. The retreat of this seaweed may significantly influence the distribution of correlated species, community structure, and ecosystem function. To date, benthic *S. horneri* populations are hardly observed in the ECS and the South China Sea, and conservation and restoration strategies are urgently required to preserve *Sargassum* forests and their associated biodiversity.

In conclusion, mtDNA data revealed two distinct lineages and limited connectivity of *Sargassum horneri* in the Chinese marginal seas. Besides, floating samples were characterized by mixed lineages, implying multiple donors. In future work, more attached samples, especially in the East/South China Sea, should be included to find the exact locations of the origin of floating populations. Besides, integration of markers from other genomes (e.g., chloroplast and nuclear) and genome-scale genotyping using SSRs or SNPs in *S. horneri* study are also needed to reveal population structure at a finer scale, and further contribute to a better understanding of how environmental shifts and biological features underpin population structuring and connectivity across seas.

This study was jointly supported by the National Key Research and Development Program of China (2016YFC1402106), the Shandong Provincial Natural Science Foundation, China (ZR201807120023), the National Natural Science Foundation of China (3170327), the Natural Science Foundation of Jiangsu Province (BK20170863), the Fundamental Research Funds for the Central Universities (B200202140), and the Key Research and Development Program of Yantai (2018ZHGY082). We also thank Sheng-Zhi Xiao, Rui-Qi Xie, Zhan-Wei Zhao, and Qing-Hai Sun for assisting in sample collection and processing. We are grateful to editors and two anonymous referees for providing valuable comments that improved the manuscript.

CONFLICT OF INTEREST

There is no conflict of interest among the authors of this article.

Assis, J., Coelho, N. C., Lamy, T., Valero, M., Alberto, F. & Serrão, E. Á. 2015. Deep reefs are climatic refugia for genetic diversity of marine forests. *J. Biogeogr.* 43:833–44.

Bandelt, H. J., Forster, P. & Röhl, A. 1999. Median-joining networks for inferring intraspecific phylogenies. *Mol. Biol. Evol.* 16:37–48.

Benzie, J. A. H. & Williams, S. T. 1997. Genetic structure of giant clam (*Tridacna maxima*) populations in the west Pacific is not consistent with dispersal by present-day ocean currents. *Evolution* 51:768–83.

Boo, G., Mansilla, A., Nelson, W., Bellgrove, A. & Boo, S. 2014. Genetic connectivity between trans-oceanic populations of *Capreolia implexa* (Gelidiales, Rhodophyta) in cool temperate waters of Australasia and Chile. *Aquat. Biol.* 119:73–9.

Bouckaert, R., Heled, J., Kuhnert, D., Vaughan, T., Wu, C. H., Xie, D., Suchard, M. A., Rambaut, A. & Drummond, A. J. 2014. BEAST 2: a software platform for bayesian evolutionary analysis. *PLoS Comput. Biol.* 10:e1003537.

Bouza, N., Caujapé-Castells, J., González-Pérez, M. A. & Sosa, P. A. 2006. Genetic structure of natural populations in the red algae *Gelidium canariense* (Gelidiales, Rhodophyta) investigated by random amplified polymorphic DNA (RAPD) markers. *J. Phycol.* 42:304–11.

Byeon, S. Y., Oh, H. J., Kim, S., Yun, S. H., Kang, J. H., Park, S. R. & Lee, H. J. 2019. The origin and population genetic structure of the 'golden tide' seaweeds, *Sargassum horneri*, in Korean waters. *Sci. Rep.* 9:7757.

Chan, S. W., Cheang, C. C., Chirapart, A., Gerung, G., Tharith, C. & Ang, P. 2013. Homogeneous population of the brown alga *Sargassum polycystum* in Southeast Asia: possible role of recent expansion and asexual propagation. *PLoS ONE* 8: e77662.

Cheang, C. C., Chu, K. H. & Ang, P. O. 2010a. Phylogeography of the marine macroalga *Sargassum hemiphyllum* (Phaeophyceae, Heterokontophyta) in northwestern Pacific. *Mol. Ecol.* 19:2933–48.

Cheang, C. C., Chu, K. H., Fujita, D., Yoshida, G., Hiraoka, M., Critchley, A., Choi, H. G., Duan, D., Serisawa, Y. & Ang, P. O. 2010b. Low genetic variability of *Sargassum muticum* (Phaeophyceae) revealed by a global analysis of native and introduced populations. *J. Phycol.* 46:1063–74.

Couceiro, L., Maneiro, I., Ruiz, J. M. & Barreiro, R. 2011. Multiscale genetic structure of an endangered seaweed *Ahnfeltiopsis pusilla* (Rhodophyta): implications for its conservation. *J. Phycol.* 47:259–68.

Ding, X., Zhang, J., Zhuang, M., Kang, X., Zhao, X., He, P., Liu, S., Liu, J., Wen, Y., Shen, H. & Zhong, J. 2019. Growth of *Sargassum horneri* distribution properties of golden tides in the Yangtze Estuary and adjacent waters. *Mar. Fisheries* 41:188–96.

Dong, Y. W., Wang, H. S., Han, G. D., Ke, C. H., Zhan, X., Nakano, T. & Williams, G. A. 2012. The impact of Yangtze River discharge, ocean currents and historical events on the biogeographic pattern of *Cellana toreuma* along the China Coast. *PLoS ONE* 7:e36178.

Duarte, B., Martins, I., Rosa, R., Matos, A. R., Roleda, M. Y., Reusch, T. B. H., Engelen, A. H. et al. 2018. Climate change impacts on seagrass meadows and macroalgal forests: an integrative perspective on acclimation and adaptation potential. *Front. Mar. Sci.* 5:190.

Duffy, J. E., Benedetti-Cecchi, L., Trinanes, J., Muller-Karger, F. E., Ambo-Rappe, R., Bostrom, C., Buschmann, A. H. et al. 2019. Toward a coordinated global observing system for Seagrasses and marine macroalgae. *Front. Mar. Sci.* 6:317.

Epstein, G. & Smale, D. A. 2017. *Undaria pinnatifida*: a case study to highlight challenges in marine invasion ecology and management. *Ecol. Evol.* 7:8624–42.

Excoffier, L., Hofer, T. & Foll, M. 2009. Detecting loci under selection in a hierarchically structured population. *Heredity* 103:285–98.

Excoffier, L. & Lischer, H. E. L. 2010. Arlequin suite ver 3.5: a new series of programs to perform population genetics analyses under Linux and Windows. *Mol. Ecol. Resour.* 10:564–7.

Faugeron, S., Valero, M., Destombe, C., Martinez, E. A. & Correa, J. A. 2001. Hierarchical spatial structure and discriminant analysis of genetic diversity in the red alga *Mazzaella laminarioides* (Gigartinales, Rhodophyta). *J. Phycol.* 37:705–16.

Fraser, C. I., Morrison, A. K., Hogg, A. M., Macaya, E. C., van Sebille, E., Ryan, P. G., Padovan, A., Jack, C., Valdivia, N. & Waters, J. M. 2018. Antarctica's ecological isolation will be broken by storm-driven dispersal and warming. *Nat. Clim. Chang.* 8:704–8.

Fraser, C. I., Zuccarello, G. C., Spencer, H. G., Salvatore, L. C., Garcia, G. R. & Waters, J. M. 2013. Genetic affinities between trans-oceanic populations of non-buoyant macroalgae in the high latitudes of the Southern Hemisphere. *PLoS ONE* 8: e69138.

Fu, Y. X. 1997. Statistical tests of neutrality of mutations against population growth, hitchhiking and background selection. *Genetics* 147:915–25.

Grummer, J. A., Beheregaray, L. B., Bernatchez, L., Hand, B. K., Luikart, G., Narum, S. R. & Taylor, E. B. 2019. Aquatic landscape genomics and environmental effects on genetic variation. *Trends Ecol. Evol.* 34:641–54.

Guillemin, M. L., Valero, M., Faugeron, S., Nelson, W. & Destombe, C. 2014. Tracing the trans-Pacific evolutionary history of a domesticated seaweed (*Gracilaria chilensis*) with archaeological and genetic data. *PLoS ONE* 9:e114039.

Guindon, S., Dufayard, J. F., Lefort, V., Anisimova, M., Hordijk, W. & Gascuel, O. 2010. New algorithms and methods to estimate maximum-likelihood phylogenies: assessing the performance of PhyML 3.0. *Syst. Biol.* 59:307–21.

Hall, T. A. 1999. BioEdit: a user-friendly biological sequence alignment editor and analysis program for Window 95/98/NT. *Nucl. Acids. Symp. Ser.* 41:95–8.

Harley, C. D. G., Anderson, K. M., Demes, K. W., Jorve, J. P., Kordas, R. L., Coyle, T. A. & Graham, M. H. 2012. Effects of climate change on global seaweed communities. *J. Phycol.* 48:1064–78.

van Hees, D. H., Olsen, Y. S., Mattio, L., Ruiz-Montoya, L., Wernberg, T. & Kendrick, G. A. 2019. Cast adrift: physiology and dispersal of benthic *Sargassum spinuligerum* in surface rafts. *Limnol. Oceanogr.* 64:526–40.

Hernández-Carmona, G., Hughes, B. & Graham, M. H. 2006. Reproductive longevity of drifting kelp *Macrocystis pyrifera* (Phaeophyceae) in Monterey Bay, USA. *J. Phycol.* 42:1199–207.

Hey, J. 2010. Isolation with migration models for more than two populations. *Mol. Biol. Evol.* 27:905–20.

Hey, J. & Nielsen, R. 2007. Integration within the Felsenstein equation for improved Markov chain Monte Carlo methods in population genetics. *Proc. Natl. Acad. Sci. USA* 104:2785–90.

Hoarau, G., Coyer, J. A., Veldsink, J. H., Stam, W. T. & Olsen, J. L. 2007. Glacial refugia and recolonization pathways in the brown seaweed *Fucus serratus*. *Mol. Ecol.* 16:3606–16.

Hu, Z. M., Li, J. J., Sun, Z. M., Gao, X., Yao, J. T., Choi, H. G., Endo, H. & Duan, D. L. 2017. Hidden diversity and phylogeographic history provide conservation insights for the edible seaweed *Sargassum fusiforme* in the Northwest Pacific. *Evol. Appl.* 10:366–78.

Hu, Z. M., Li, J. J., Sun, Z. M., Oak, J. H., Zhang, J., Fresia, P., Grant, W. S. & Duan, D. L. 2015. Phylogeographic structure and deep lineage diversification of the red alga *Chondrus ocellatus* Holmes in the Northwest Pacific. *Mol. Ecol.* 24:5020–33.

Hu, Z. M., Uwai, S., Yu, S. H., Komatsu, T., Ajisaka, T. & Duan, D. L. 2011. Phylogeographic heterogeneity of the brown macroalga *Sargassum horneri* (Fucaceae) in the northwestern Pacific in relation to late Pleistocene glaciation and tectonic configurations. *Mol. Ecol.* 20:3894–909.

Kaplanis, N. J., Harris, J. L. & Smith, J. E. 2016. Distribution patterns of the non-native seaweeds *Sargassum horneri* (Turner) C. Agardh and *Undaria pinnatifida* (Harvey) Suringar on the San Diego and Pacific coast of North America. *Aquat. Invasions* 11:111–24.

Komatsu, T., Fukuda, M., Mikami, A., Mizuno, S., Kantachumpoo, A., Tanoue, H. & Kawamiya, M. 2014a. Possible change in distribution of seaweed, *Sargassum horneri*, in northeast Asia under A2 scenario of global warming and consequent effect on some fish. *Mar. Pollut. Bull.* 85:317–24.

Komatsu, T., Mizuno, S., Natheer, A., Kantachumpoo, A., Tanaka, K., Morimoto, A., Hsiao, S. T., Rothäusler, E. A., Shishidou,

H., Aoki, M. & Ajisaka, T. 2014b. Unusual distribution of floating seaweeds in the East China Sea in the early spring of 2012. *J. Appl. Phycol.* 26:1169–79.
Komatsu, T., Tatsukawa, K., Filippi, J. B., Sagawa, T., Matsunaga, D., Mikami, A., Ishida, K. et al. 2007. Distribution of drifting seaweeds in eastern East China Sea. *J. Mar. Syst.* 67:245–52.
Le Cam, S., Daguin-Thiebaut, C., Bouchemousse, S., Engelen, A. H., Mieszkowska, N. & Viard, F. 2019. A genome-wide investigation of the worldwide invader *Sargassum muticum* shows high success albeit (almost) no genetic diversity. *Evol. Appl.* 13:500–14.
Li, J. J., Hu, Z. M., Gao, X., Sun, Z. M., Choi, H. G., Duan, D. L. & Endo, H. 2017a. Oceanic currents drove population genetic connectivity of the brown alga *Sargassum thunbergii* in the north-west Pacific. *J. Biogeogr.* 44:230–42.
Li, J. J., Hu, Z. M., Sun, Z. M., Yao, J. T., Liu, F. L., Fresia, P. & Duan, D. L. 2017b. Historical isolation and contemporary gene flow drive population diversity of the brown alga *Sargassum thunbergii* along the coast of China. *BMC Evol. Biol.* 17:10.
Lin, S. M., Huang, R., Ogawa, H., Liu, L. C., Wang, Y. C. & Chiou, Y. 2017. Assessment of germling ability of the introduced marine brown alga, *Sargassum horneri*, in Northern Taiwan. *J. Appl. Phycol.* 29:2641–9.
Liu, F., Liu, X., Wang, Y., Jin, Z., Moejes, F. W. & Sun, S. 2018. Insights on the *Sargassum horneri* golden tides in the Yellow Sea inferred from morphological and molecular data. *Limnol. Oceanogr.* 63:1762–73.
Macaya, E. C. & Zuccarello, G. C. 2010. Genetic structure of the giant kelp *Macrocystis pyrifera* along the southeastern Pacific. *Mar. Ecol. Prog. Ser.* 420:103–12.
Miller, K. A., Engle, J. M., Uwai, S. & Kawai, H. 2007. First report of the Asian seaweed *Sargassum filicinum* Harvey (Fucales) in California, USA. *Biol. Invasions* 9:609–13.
Muhlin, J. F. & Brawley, S. H. 2009. Recent versus relic: discerning the genetic signature of *Fucus vesiculosus* (Heterokontophyta; Phaeophyceae) in the northwestern Atlantic. *J. Phycol.* 45:828–37.
Neiva, J., Pearson, G. A., Valero, M. & Serrão, E. A. 2012. Drifting fronds and drifting alleles: range dynamics, local dispersal and habitat isolation shape the population structure of the estuarine seaweed *Fucus ceranoides*. *J. Biogeogr.* 39:1167–78.
Ng, P. K., Chiou, Y. S., Liu, L. C., Sun, Z., Shimabukuro, H. & Lin, S. M. 2019. Phylogeography and genetic connectivity of the marine macro-alga *Sargassum ilicifolium* (Phaeophyceae, Ochrophyta) in the northwestern Pacific. *J. Phycol.* 55:7–24.
Ni, G., Li, Q., Kong, L. F. & Yu, H. 2014. Comparative phylogeography in marginal seas of the northwestern Pacific. *Mol. Ecol.* 23:534–48.
Nielsen, R. & Wakeley, J. 2001. Distinguishing migration from isolation: a Markov chain Monte Carlo approach. *Genetics* 158:885–96.
Pang, Y., Liu, Z., Ding, L., Fu, W., Yu, S., Sun, Z. & Qin, S. 2018. Morphological comparison and analysis of the vesicle and receptacle of floating and attached *Sargassum horneri* in Shandong peninsula. *Mar. Sci.* 42:84–91.
Peakall, R. & Smouse, P. E. 2012. GenAlEx 6.5: genetic analysis in Excel. Population genetic software for teaching and research-an update. *Bioinformatics* 28:2537–9.
Posada, D. & Crandall, K. A. 1998. MODELTEST: testing the model of DNA substitution. *Bioinformatics* 14:817–8.
Provan, J. 2013. The effects of past, present and future climate change on range-wide genetic diversity in northern North Atlantic marine species. *Front. Biogeogr.* 5:60–6.
Qi, L., Hu, C., Wang, M., Shang, S. & Wilson, C. 2017. Floating algae blooms in the East China Sea. *Geophys. Res. Lett.* 44:11501–9.
Reusch, T. B. H. 2014. Climate change in the oceans: evolutionary versus phenotypically plastic responses of marine animals and plants. *Evol. Appl.* 7:104–22.
Rogers, A. R. & Harpending, H. 1992. Population growth makes waves in the distribution of pairwise genetic differences. *Mol. Biol. Evol.* 9:552–69.
Ronquist, F., Teslenko, M., van der Mark, P., Ayres, D. L., Darling, A., Höhna, S., Larget, B., Liu, L., Suchard, M. A. & Huelsenbeck, J. P. 2012. MrBayes 3.2: efficient Bayesian phylogenetic inference and model choice across a large model space. *Syst. Biol.* 61:539–42.
Rothäusler, E., Corell, H. & Jormalainen, V. 2015. Abundance and dispersal trajectories of floating *Fucus vesiculosus* in the Northern Baltic Sea. *Limnol. Oceanogr.* 60:2173–84.
Saunders, G. W. 2014. Long distance kelp rafting impacts seaweed biogeography in the northeast Pacific: the kelp conveyor hypothesis. *J. Phycol.* 50:968–74.
Sissini, M. N., Barbosa de Barros Barreto, M. B., Menezes Szechy, M. T., de Lucena, M. B., Oliveira, M. C., Gower, J., Liu, G. et al. 2017. The floating *Sargassum* (Phaeophyceae) of the South Atlantic Ocean – likely scenarios. *Phycologia* 56:321–8.
Su, L., Shan, T., Pang, S. & Li, J. 2017. Analyses of the genetic structure of *Sargassum horneri* in the Yellow Sea: implications of the temporal and spatial relations among floating and benthic populations. *J. Appl. Phycol.* 30:1417–24.
Tajima, F. 1989. Statistical method for testing the neutral mutation hypothesis by DNA polymorphism. *Genetics* 123:585–95.
Tala, F., Lopez, B. A., Velasquez, M., Jeldres, R., Macaya, E. C., Mansilla, A., Ojeda, J. & Thiel, M. 2019. Long-term persistence of the floating bull kelp *Durvillaea antarctica* from the South-East Pacific: potential contribution to local and transoceanic connectivity. *Mar. Environ. Res.* 149:67–79.
Thompson, J. D., Gibson, T. J., Plewniak, F., Jeanmougin, F. & Higgins, D. G. 1997. The CLUSTAL_X windows interface: flexible strategies for multiple sequence alignment aided by quality analysis tools. *Nucleic Acids Res.* 25:4876–82.
Uwai, S., Kogame, K., Yoshida, G., Kawai, H. & Ajisaka, T. 2009. Geographical genetic structure and phylogeography of the *Sargassum horneri/filicinum* complex in Japan, based on the mitochondrial cox3 haplotype. *Mar. Biol.* 156:901–11.
Wang, J., Tsang, L. M. & Dong, Y. W. 2015. Causations of phylogeographic barrier of some rocky shore species along the Chinese coastline. *BMC Evol. Biol.* 15:114.
Waters, J. M., Fraser, C. I. & Hewitt, G. M. 2013. Founder takes all: density-dependent processes structure biodiversity. *Trends in Ecol. Evol.* 28:78–85.
Wernberg, T., Bennett, S., Babcock, R. C., de Bettignies, T., Cure, K., Depczynski, M., Dufois, F. et al. 2016. Climate-driven regime shift of a temperate marine ecosystem. *Science* 353:169–72.
Xing, Q. G., Guo, R. H., Wu, L. L., An, D. Y., Cong, M., Qin, S. & Li, X. R. 2017. High-resolution satellite observations of a new hazard of golden tides caused by floating *Sargassum* in winter in the Yellow Sea. *IEEE Geosci. Remote Sens. Lett.* 14:1815–9.
Xu, J. W., Chan, T. Y., Tsang, L. M. & Chu, K. H. 2009. Phylogeography of the mitten crab *Eriocheir sensu* stricto in East Asia: pleistocene isolation, population expansion and secondary contact. *Mol. Phylogenet. Evol.* 52:45–56.
Xu, M., Sakamoto, S. & Komatsu, T. 2016. Attachment strength of the subtidal seaweed *Sargassum horneri* (Turner) C. Agardh varies among development stages and depths. *J. Appl. Phycol.* 28:3679–87.
Xu, M., Sasa, S. & Komatsu, T. 2018. *Sargassum horneri* C. Agardh space capacity estimation reveals that thallus surface area varies with wet weight. *PLoS ONE* 13:e0199103.
Xuereb, A., Benestan, L., Normandeau, E., Daigle, R. M., Curtis, J. M. R., Bernatchez, L. & Fortin, M. J. 2018. Asymmetric oceanographic processes mediate connectivity and population genetic structure, as revealed by RADseq, in a highly dispersive marine invertebrate (*Parastichopus californicus*). *Mol. Ecol.* 27:2347–64.
Yatsuya, K. 2008. Floating period of *Sargassacean thalli* estimated by the change in density. *J. Appl. Phycol.* 20:797–800.
Yoshida, G., Arima, S. & Terawaki, T. 1998. Growth and maturation of the 'autumn-fruiting type' of *Sargassum horneri* (Fucales, Phaeophyta) and comparisons with the 'spring-fruiting type'. *Phycol. Res.* 46:183–9.
Yu, S., Chong, Z., Zhao, F., Yao, J. & Duan, D. 2013. Population genetics of *Sargassum horneri* (Fucales, Phaeophyta) in China

revealed by ISSR and SRAP markers. *Chinese J. Oceanol. Limnol.* 31:609–16.

Zhang, J., Shi, J., Gao, S., Huo, Y., Cui, J., Shen, H., Liu, G. & He, P. 2019. Annual patterns of macroalgal blooms in the Yellow Sea during 2007–2017. *PLoS ONE* 14:e0210460.

Zhang, J., Yao, J. T., Sun, Z. M., Fu, G., Galanin, D. A., Nagasato, C., Motomura, T., Hu, Z. M. & Duan, D. L. 2015. Phylogeographic data revealed shallow genetic structure in the kelp *Saccharina japonica* (Laminariales, Phaeophyta). *BMC Evol. Biol.* 15:12.

Zhu, Q., Ren, J., Chen, J. & Yang, R. 2019. The morphological and ultrastructural profiling between floating and benthic *Sargassum horneri*. *J. Biol.* 36:51–4.

Supporting Information

Additional Supporting Information may be found in the online version of this article at the publisher's web site:

Figure S1 Geographical distribution of haplotypes (a) of *Sargassum horneri* and rooted BI/ML trees inferred from each mtDNA RPL (b), RNL (c) and COB (d) locus. Posterior probabilities/bootstrap support from the maximum likelihood analyses are shown near each node (only values higher than 0.70/70 are shown). Dash lines represent outgroup clade (*Sargassum natans* KY084907.1, *S. fluitans* KY084909.1 and *S. muticum* KJ938301.1). Numbers in the pie chart correspond to the sampling localities in Table S1. Blue and yellow colors represent the proportion of lineages respectively in each population.

Table S1 Genetic diversity indices of *Sargassum horneri* populations inferred from concatenated data mtDNA RPL+MLA+COB. *n*, number of sequences; N_h, number of haplotypes; H_p, number of private haplotypes; *h*, haplotype diversity; π, nucleotide diversity.

Table S2 Variable nucleotides in the mitochondrial RPL+RNL+COB haplotypes of *Sargassum horneri*. Variable sites from RPL were marked with r1-4; Variable sites from RNL were marked with n1-3; Variable sites from COB were marked with c1-6. Haplotypes and lineages are identical to Figure 1.

Table S3 Haplotype distribution in benthic and floating *Sargassum horneri* samples in the Chinese marginal seas based on concatenated mtDNA sequences. L1 (%), percent of sequences in lineage I; L2 (%), percent of sequences in lineage II.

Table S4 Genetic diversity indices of benthic and floating *Sargassum horneri* in the Chinese marginal seas inferred from mtDNA *rpl5-rps3* (RPL), *rnl-atp9* (RNL) and *cob-cox2* (COB). *n*, number of sequences; N_h, number of haplotypes; *h*, haplotype diversity; π, nucleotide diversity.

Table S5 Pairwise values of F_{ST} between benthic and floating *Sargassum horneri* populations based on concatenated mtDNA sequences. Boldface indicates that values are significant ($P < 0.05$). Numbers correspond to the sampling localities in Table S1 and Figure 1.